Theoretical Chemistry Accounts (2023) 142:87
https://doi.org/10.1007/s00214-023-03022-8

RESEARCH

Electron density analysis on the alpha acidity of nitriles

José Luis López[1] · Filipe Teixeira[2] · Ana M. Graña[1] · Ricardo A. Mosquera[1]

Received: 29 April 2023 / Accepted: 13 July 2023 / Published online: 18 August 2023

Abstract
24 substituted cyanocompounds and the corresponding anions obtained upon H^+-abstraction from diverse positions were subjected to an electron density analysis with the quantum theory of atoms in molecules (QTAIM). All the electron densities were obtained at the B3LYP/6–31 + + G(2d,2p) level on completely optimized geometries. In accordance to experimental evidence, α-H^+ abstraction is found as the most favored one (by at least 100 kJ mol^{-1} in all the tested compounds). The presence of additional resonance electron attractors reduces significantly the α-deprotonation energy, whereas this magnitude is quite insensitive to the inclusion of resonance electron donors. The electron density rearrangement accompanying the deprotonation is apparently in line with the predictions of the resonance model (RM). In fact, a significant part of the electron density gained by expelling the proton is transferred to cyano N and to other groups where significant resonance structures delocalize the negative charge. Nevertheless, some significant modifications have to be introduced on the RM picture when the QTAIM results are studied in detail.

Keywords Nitriles · Deprotonation · Acidity · QTAIM

1 Introduction

Carbanions stabilized by mesomeric electron acceptor groups are a class of compounds with a certain practical interest. In fact, they have been employed widely in organic synthesis [1]. Even, some important biochemical intermediates display this chemical moiety [2]. From a theoretical point of view, they are convenient systems for testing the reliability of electron delocalization models. According to the resonance model (RM), the negative charge of the C atom is expected to be delocalized on the mesomeric electron acceptor, *e.g.* O in a carbonyl group or N in a cyano substituent. In this context, we acknowledge the very good services provided by RM in chemistry [3, 4]. Even, different possibilities to supply resonance structures with more reliable and quantitative weighting coefficients obtained making use of modern tools of electron density topological analysis can be explored [5]. Nevertheless, since the publication of the seminal paper by Wiberg and Laidig on the electronic origin of the esther and amide resonance [6], it is not possible to deny that a large amount of inconsistencies between RM predictions and computed evolutions of electron densities have been reported [7–26]. Most of these discrepancies were obtained by studying protonation processes or in nucleophilic addition reactions. In contrast, deprotonations seem to have been much less explored.

This paper aims to get insight into the stabilization of carbanions by cyano groups that is on the basis of the significant acidity displayed by the hydrogens of methylenes (and other groups) that are α to CN units. In order to achieve this objective, we have performed an electron density analysis of neutral and deprotonated anionic species of a series of substituted N≡CHRR' cyanocompounds (R' = H in most of them) (Table 1). This analysis was carried out with the quantum theory atoms in molecules (QTAIM) [21, 27] on gas phase optimized structures. We are aware that H-abstraction usually takes place in aqueous media; nevertheless, being our main interest electron density evolutions, we have opted for studying this process in isolated molecules to avoid any possible effect of solvation models on the reliability of electron densities.

✉ Ana M. Graña
ana@uvigo.gal

✉ Ricardo A. Mosquera
mosquera@uvigo.es

[1] Dpto. Química Física, Universidade de Vigo, Lagoas-Marcosende, 36310 Vigo, Galicia, Spain

[2] LAQV-REQUIMTE, Faculty of Sciences, University of Porto, Rua do Campo Alegre, 4169-007 Porto, Portugal

Table 1 Deprotonation energies, $\Delta_{dp}E$ (in kJ mol^{-1}) and accuracy estimators for QTAIM integrations for the RR'CH–C≡N molecules here studied[a]

	R	R'	$\Delta_{dp}E$	$\Delta\Delta_{dp}E$	ω	$\Sigma N(\Omega)$-N[c]	$\Sigma E(\Omega)$-E[d]	$\lvert L(\Omega)\rvert$[e]
1	H	H	1549.3	0	152.8	0.8 (– 0.1)[f]	0.3 (0.0)[f]	0.1 (0.1)
2	H	CN	1375.6	– 173.7	179.9	0.6 (0.5)	0.3 (0.3)	0.2 (0.2)
3	CN	CN	1228.9	– 320.4	180.0	0.2 (0.2)	0.1 (0.2)	0.1 (0.1)
4	CH_3–O–CO	H	1402.2	– 147.1	180.0	2.1 (2.0)	1.1 (1.5)	1.3 (1.9)
5	NO_2	H	1334.4	– 214.9	179.8	0.9 (1.8)	0.8 (1.4)	1.5 (1.8)
6	OH	H	1547.3	– 2	128.7	– 0.4 (0.0)	– 0.3 (– 0.1)	0.1 (0.6)
7	NH_2	H	1552.2	2.9	151.6	0.6 (– 0.7)	0.4 (– 0.3)	0.8 (0.2)
8	Li	H	1660.7	111.4	164.3			
9	SiH_3	H	1472.0	– 77.3	180.0	– 0.9 (– 1.1)	– 4.3 (– 3.5)	2.0 (1.7)
10	F	H	1526.6	– 22.7	120.6	– 0.5 (– 1.2)	– 0.3 (– 0.6)	0.2 (0.7)
11	F	F	1503.4	– 45.9	109.4	– 0.6 (– 0.3)	– 0.1 (– 0.2)	1.8 (0.4)
12	CH_3	H	1558.8	9.5	150.3	0.7 (0.7)	0.5 (0.0)	1.1 (0.4)
13	CH_3	CH_3	1556.6	7.3	148.6	1.2 (2.0)	0.8 (0.7)	0.9 (0.8)
14	$CH_3(CH_2)_8$	H	1548.0	– 1.3	167.1	– 0.4 (1.0)	7.7 (2.0)	4.1 (1.0)
15	$CH_3(CH_2)_9$	H	1548.2	– 1.1	167.9	0.4 (0.8)	– 1.8(1.1)	0.9 (0.8)
16[b]	CH_2=CH–CN	–	1548.4	– 0.9	180.0	0.1 (– 0.6)	0.1 (– 0.3)	0.4 (0.4)
17	CH_2=CH	H	1458.0	– 91.3	179.9	0.0 (0.8)	0.0 (0.7)	0.3 (1.3)
18	C_6H_5	H	1444.2	– 105.1	180.0	0.6 (0.5)	0.4 (0.3)	0.5 (0.6)
19	*p*–$NO_2C_6H_4$	H	1342.6	– 206.7	180.0	0.3 (– 0.2)	1.2 (1.5)	0.8 (1.6)
20	*p*-$NH_2C_6H_4$	H	1469.5	– 79.8	179.8	– 0.1 (– 0.1)	0.3 (1.0)	0.4 (0.9)
21	*m*-$NO_2C_6H_4$	H	1388.5	– 161	179.9	2.2 (0.7)	1.2 (0.4)	1.6 (0.4)
22	*m*-$NH_2C_6H_4$	H	1453.6	– 95.8	180.0	0.8 (1.3)	0.6 (0.7)	0.4 (0.5)
23	*o*-$NO_2C_6H_4$	H	1363.0	– 186.3	180.0	– 0.3 (1.2)	– 0.2 (0.7)	0.8
24	*o*-$NH_2C_6H_4$	H	1455.5	– 93.8	170.7	0.2 (0.4)	0.1 (0.1)	0.9

[a]Values for deprotonated species in parenthesis

[b]This compound, CH_2=CH–CN, does not follow the general RR'CH–CN formula

[c]Values in au multiplied by 10^3

[d]in kJ mol^{-1}

[e]Maximum absolute value of integrated $L(\Omega)$ in the neutral molecule and its protonated species, in au multiplied by 10^3

As starting point, we remind that N≡C$^-$RR' anions are considered to be stabilized by delocalization of the negative charge on the N atom. This is represented by $^-$N≡CRR' resonance Lewis structures. In polysubstituted nitriles, delocalizations can be extended to other atoms of R and R' groups where similar resonance structures could be written. Scheme 1 shows an example of them for compound **5**, which contains an additional π-acceptor substituent: NO_2. The opposite effect should be expected when the additional substituent is a π-donor like -NH_2 or –OH.

1.1 Computational details

QTAIM allows the partitioning of a molecule into disjoint subsystems without resorting to hypothesis alien to quantum mechanics [21, 27]. With a few exceptions [29], each of these subsystems consists of a nucleus, which acts as an attractor for the trajectories of the gradient of the electron density vector field, $\nabla\rho(\boldsymbol{r})$, and its associated atomic basin, throughout these trajectories spread. An atom, Ω,

Scheme 1 Resonance Lewis structures for the anion of compound 5

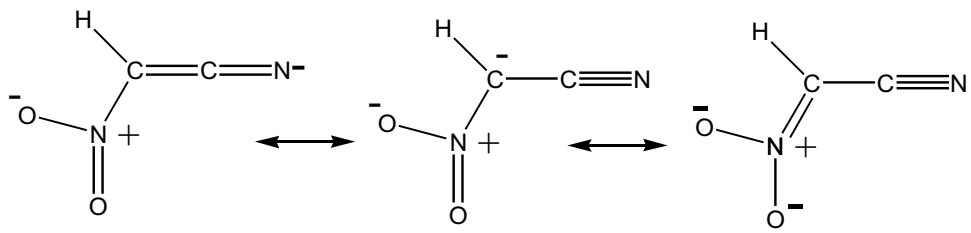

is defined as the union of the attractor and its associated basin, and is surrounded by zero flux surfaces for $\nabla\rho(\boldsymbol{r})$. The integration of the proper density functions within these limits provides diverse atomic properties such as the electron population, $N(\Omega)$, or the total atomic electron energy, $E(\Omega)$.

QTAIM also recovers main elements of molecular structure in terms of the critical points, $\boldsymbol{r}_c$, of the electron density, $\rho(\boldsymbol{r})$. Prominent among them are the bond critical points (BCPs), which are located roughly in between every pair of bonded atoms. The electron density at a certain BCP is regarded as an indicator for bond strength within a homologous series.

All the neutral (**1**–**24**) and deprotonated (**1a**-**24a**) species here considered (Table 1) were fully optimized at the B3LYP/6–31 + + G(2d,2p) levels using the Gaussian-09 program [22]. Excluding the long chain linear cyanoalkanes (**14** and **15**), initial geometries were optimized for all expected conformers. The completely antiperiplanar conformation was the only initial geometry optimized for **14** and **15**. H^+-extraction on these structures gives rise to a C–C–C–CN gauche arrangement in **14a** and **15a**. Electron densities obtained were analyzed with the QTAIM by means of the program AIMPAC [23]. The accuracy of the integrated properties was tested using the differences between molecular properties and those obtained by summation of the properties of the fragments [N-$\Sigma N(\Omega)$ or E-$\Sigma E(\Omega)$] (Table 1). These differences are always smaller (in absolute value) than $2{\cdot}10^{-3}$ au and 1.2 kJ/mol, respectively, which are found to be accurate enough comparing with other works carried out at similar theoretical levels. In the same vein, the integrated values of the Laplacian of the electron density in all the atomic fragments, $L(\Omega)$, are always smaller (in absolute value) than 10^{-3} au.

Deprotonation energies, $\Delta_{dp}E$, (Table 1) were calculated taking into account the thermal and zero point vibrational corrections (unscaled) obtained for deprotonated and neutral species. All the optimized structures were real minima as they do not display any imaginary frequency. When more than one local minimum is present in the neutral or anionic form of a certain compound, $\Delta_{dp}E$ is computed as the different between the lowest energy conformer found for each species.

2 Results and discussion

Atomic and bond properties of neutral nitriles, as well as the $\nabla^2\rho(\boldsymbol{r})$ topology, have been described thoroughly in a previous HF study by Aray et al. [24]. As our results for neutral molecules are in perfect agreement with theirs, we focus our discussion on the effects of deprotonation.

2.1 Deprotonation energies

Table 1 lists the $\Delta_{dp}E$ energies obtained for α-deprotonation of the 24 cyanocompounds here studied. For the sake of simplicity, in what follows compound **1** (cyanomethane) will be our reference, and deprotonation energies will be commented as relative values to that computed for **1** ($\Delta\Delta_{dp}E$). First we notice that, in spite of large structural changes, deprotonation energies do not span in a wide range. It is also noticeable that positive values are scarce. This is especially true when we take into account that the most positive value corresponds to $LiCH_2CN$ (compound **8**), whose neutral optimized structure is significantly different from those of the remaining species, with the Li atom attached to the CN group and not to the α methylene, denoting its ionic character. Thus, one $[CH_2CN]^-$anion is already formed in neutral **8**. As a consequence, abstracting a proton from it demands the largest amount of energy and this compound can be excluded from the series because of this singular bonding structure.

The other positive $\Delta\Delta_{dp}E$ values do not exceed 10 kJ mol^{-1} (**7**, **12** and **13**). **12** and **13** correspond to other short alkyl chains (cyanoethane and cyano-*iso*-propane). The small difference between them (Table 1) leads us to think that chain ramifications are not significant to this problem. The effect of chain size is even smaller for larger alkyl groups (**14** and **15**), becoming negligible.

7 should be compared with the other resonance electron donor containing compound (+ R) here considered: **6**. Both values are really close (slightly positive one and slightly negative the other). Thus, we conclude that the inclusion of + R substituents does not really modify $\Delta_{dp}E$.

In contrast, significantly negative $\Delta\Delta_{dp}E$ values are displayed by those compounds (**2**–**5**) that include additional (CN being also one of them) resonance electron withdrawers (-R). According to the RM, these compounds allow a larger delocalization of the formal negative charge formed at the C^{α} (Scheme 1). A similar mechanism can be considered for π-conjugated substituents, such as vinyl (**17**) of phenyl (parent, **18**, or substituted, **19**–**24**) groups. In fact, all these compounds (**2**–**5**, **17**–**24**) reduce the deprotonation energy by more than 90 kJ mol^{-1} with regard to the reference (**1**).

We have also checked that α-deprotonations are preferred over other possible processes for H^+-abstractions. To this end, we computed all possible H-abstractions along the alkyl chain of **14** and **15** (Fig. 1). Other deprotonations cost at least 100 kJ mol^{-1} more than the alpha one. Moreover, the only significant difference between both compounds is due to the displacement (by one position) of the terminal and previous to terminal methyl or methylene group.

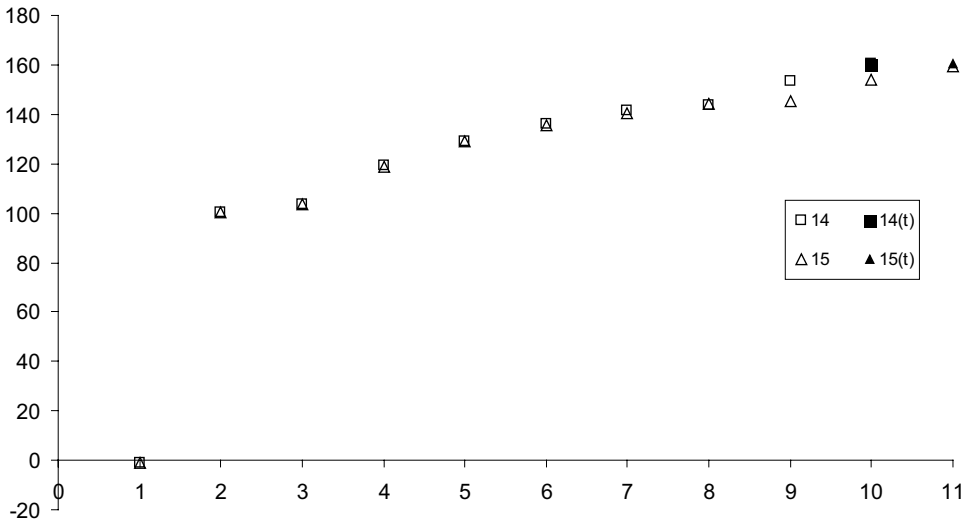

Fig. 1 Relative values (in kJ mol^{-1}) of deprotonation energies ($\Delta\Delta_{dp}E$) vs. H^+-abstraction position in compounds **14** and **15**

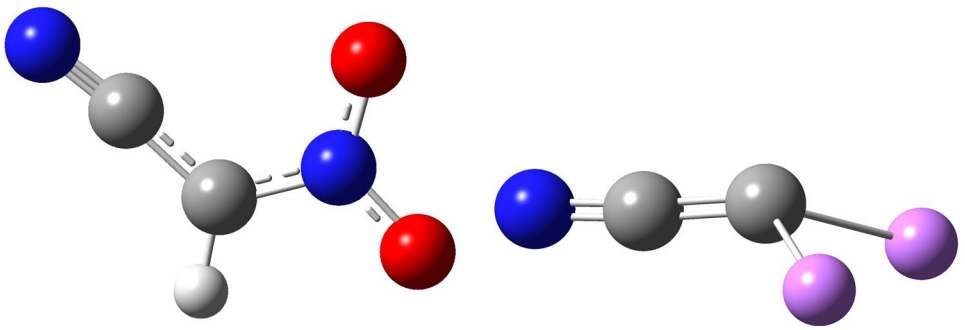

Fig. 2 Optimized structures for anions **5a** (planar) and **11a** (ω = 109.4°)

2.2 Anion geometries

Anions where the RM predicts π electron delocalization to substituent groups are found to be planar or nearly planar. This is shown by the ω dihedral angle formed between R–C–C R´− C–C units (Table 1). The unique significant exception to this trend is found in **24** (2-aminobenzylnitrile), where the steric hindrance between the non-planar NH_2. group and the hydrogen atom attached to the α-methylene prevent from a planar arrangement in the anion. In contrast, when substituents do not allow π electron delocalization the surroundings of the C atom are not planar (109° < ω < 168°) (Fig. 2). The presence of highly electronegative substituents (F or OH) coincides with the largest deviations from planarity (compounds **6a**, **10a** and **11a**).

2.3 Deprotonation effects on atomic electron populations and bond properties in cyanomethane and other alkyl nitriles

As in the previous section, we first describe the electron density change due to α-deprotonation in acetonitrile, compound **1,** taken again as our basic model. The variations

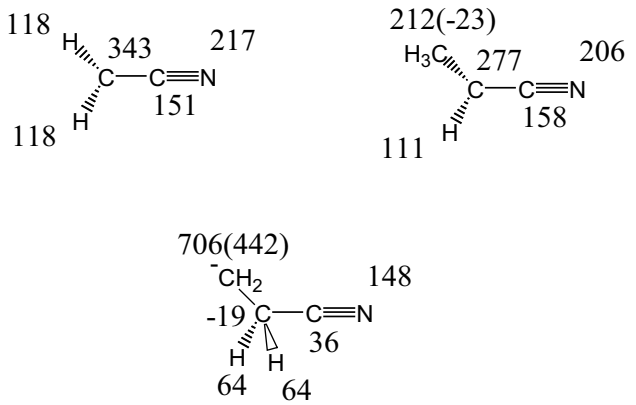

Fig. 3 Variations of atomic electron populations in **1** and **12** upon α-deprotonation and those of **12** upon the preferred β-deprotonation, $\Delta_{dp}N(\Omega)$, (in au multiplied by 10^3). $\Delta_{dp}N(\Omega)$ values for β-CH_3 or β-$^-CH_2$ groups and corresponding C (in parenthesis) are shown for **12**

experienced in the process by its atomic electron populations, $\Delta N(\Omega)$, are included in the first scheme of Fig. 3. All the atoms increase their electron population after expelling the proton, which means sharing 0.948 au. Whereas a little

more than one half of the electron density is kept within the CH_2 unit, the electron density taken by the cyano group is important, and there is an important transference of electron density to its N atom. That is, the expectations deduced from the resonance model are basically observed in the QTAIM results.

In the same vein, the evolutions of BCPs properties are in line with the predictions of the RM model. Thus, we notice (Fig. 4) the C–C bond is reinforced while the CN linkage gets weaker. At the same time, the first bond shrinks by 0.08 Å, while the later lengths by 0.03 Å. More meaningful, both bond ellipticities that are perfectly negligible in the neutral compound become 0.296 and 0.042 in the anion. Finally, the values of the total energy density function become more negative for C–C in the anion and less negative for the CN linkage, pointing to a reinforcement of covalent character in the former and to its depletion toward a significant polarization in the latter.

At least in a first glance, the electron density evolution experienced in the α-deprotonation of propanenitrile, compound **12**, seems to follow the same trends exposed for acetonitrile. In spite of the larger size of the R alkyl group, the electron population gained by the CN group is only 0.004 au lower than in **1**. We observe (Fig. 3) that the increase in electron population in the rest of the molecule is 0.021 au larger in **12** than in **1**, but most of this difference is due to the fact that the atomic electron population of H in a methylene group (0.964 au in **12**) is larger than that of a H in a methyl group (0.948 au in **1**). In contrast, more than 70% of the electron density taken from the extracted H in the β-deprotonation of propanenitrile remains in the ipso CH group (Fig. 3).

After studying compounds with larger alkyl groups, a nearly transferable general scheme (Fig. 5) can be established for the electron density reorganization associated to α-deprotonation. Thus, we can say that the electron density

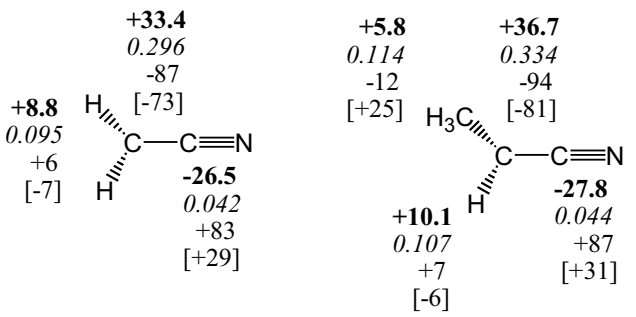

Fig. 4 Variations of most significant BCP properties in **1** and **12** upon α-deprotonation: Relative electron density values (in au and boldface) are multiplied by 10^3, absolute values of ellipticities (in italics) and relative values of the total electronic energy density (multiplied by 10^3). Variation of bondlengths (in Å multiplied by 10^3) are shown in brackets

Table 2 Variations of most significant BCP properties upon α-deprotonation in **15**

	$\Delta\varepsilon$	$10^3\Delta\rho(\boldsymbol{r}_c)$/au	$10^3\Delta H(\boldsymbol{r}_c)$/au	$10^3\Delta R$/Å
C≡N	0.045	− 27.9	87.4	30
C^{α}-C(N)	0.341	38.1	− 94.9	− 83
C^{α}-C^{β}	0.099	11.8	− 21.1	− 36
C^{α}-H	0.100	− 8.0	3.4	− 9

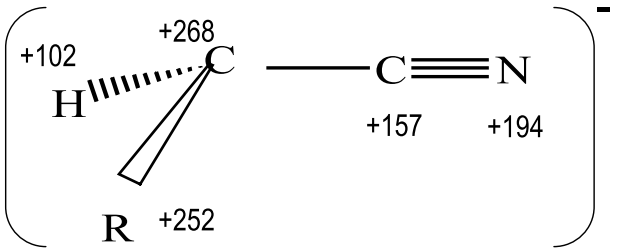

Fig. 5 Electron density reorganization accompanying α-deprotonation in alkyl nitriles **14** and **15**. All values are variation of atom/group electron populations in au multiplied by 10^3

taken from the extracted hydrogen splits into three parts: (i) that concentrated in the ipso group (0.370 au); (ii) a nearly equivalent part transferred to the cyano group (0.351 au); and (iii) that taken by the alkyl group (0.252 au). We notice that although this third part is not represented by any usual resonance form ($R^{-}CH–CN$), it is far from being negligible. Moreover, within the cyano group, the increase in electron population in both atoms is comparable. The variations experienced by the most significant BCP properties in these compounds can be represented by those around the RHC^{α}–CN unit of compound **15** (Table 2). The values point to reinforcement of the C^{α}–C(N) bond and weakening of the CN bond, and both trends are represented by the $RCH=C=N^{-}$ resonance form. There is also a noticeable reinforcement of the C^{α}–C^{β} bond, not predicted by the RM.

Finally, when the proton is extracted from a ternary carbon, as in 2-methylproapnenitrile (**13**), we notice the changes in the CN unit are certainly small with regard to the nearly transferable scheme (Fig. 5). In contrast, the electron population gained by the α C decreases to 0.215 au, as two alkyl groups are available to receive electron density (0.221 au each).

2.4 Deprotonation effects on atomic electron populations and bond properties in substituted acetonitriles (XCH_2CN; X = CN, NO_2, CH_3OCO, SiH_3, OH, NH_2, F)

The introduction of electron donors or acceptors as additional functional groups in acetonitrile modifies

significantly the reorganization of the electron density after α-deprotonation. Including additional acceptors, *e.g.* more CN groups, reduces the electron density gained at the ipso group. We observe $\Sigma\Delta N(\Omega)$ goes from 0.579 au to 0.298 au and 0.118 au in CH_2/CH/C unit as we progressively increase the number of CN groups in the series formed by compounds **1**, **2** and **3**. At the same time, the electron density gained by each CN also reduces (0.364, 0.300 and 0.247 au, respectively), while the proportion of electron density transferred to the nitrogen of each cyano group increases (59%, 68%, 78%). A similar trend is observed when two different resonance electron acceptors groups combine in the molecule (**4** and **5**). The electron density gained by the CH group in the anions of **2**, **4** and **5** (0.298 au, 0.235 au and 0.014 au), or that collected by the CN group (0.300 au, 0.255 au and 0.235 au, respectively) can be taken as an estimator for the relative strength of CN, CH_3OCO and NO_2 groups. The larger the diminution, the stronger the electron acceptor ability.

The presence of electron donors, like OH or NH_2 groups, hampers spreading the electron density along the molecule. Figure 6 compares the effects, drastically different in CH area, introduced by α-deprotonation in cyanocompounds containing the strongest electron acceptor (NO_2, compound **5**) and the strongest electron donor (OH, compound **6**).

Fluorine atoms are considered sometimes as subtle substituents, able to act both as electron donors (through resonance) or acceptors (because of their high electronegativity). We have computed $\Delta N(\Omega)$ values for compounds **10** and **11**. The results indicate that, in what regards electron reorganization related to α-deprotonation, fluorine behavior closely resembles that of strong donors. Moreover, the anions of **10** and **11** are not planar, as it is found for those containing OH or NH_2 groups.

The variation experienced by the most significant BCP properties for the compounds in this series is summarized in Table 3. C^{α}–R bonds display an opposite behavior when we compare compounds enclosing electron donors (**6**), where the C^{α}–R bond is slightly weaker in the anion, and electron acceptors (**5**), where it gets stronger. According to these properties, fluorine (see compound **10**) also behaves as an electron donor. We also notice that N–O bonds length (Table 3) upon α-deprotonation, as predicted by the RM.

Finally, silicon is attached to the α methylene group in compound **9**. This allows to test if this substituent works as an electron acceptor as it is usually stated invoking the "empty d orbitals" in Si. Surprisingly, the electron population of the silicon atom does not change in the process (Fig. 7), and the electron density reorganization observed is more alike that of strong electron donors. Nevertheless, the HC–CN arrangement in the anion is perfectly planar, like those presented by strong electron acceptors. Moreover, looking at BCP properties, we observe the C-Si bond reinforces in the anion with regard to neutral compound **9** (Table 3). Certainly, this trend is not so neat as in nitroso-compound **5**, but it is significantly larger than in cyanoalkanes (Table 2). It is also found that Si–H bonds weaken to a different extension depending on their arrangement (gauche or anti) with regard to the CN group. This trend is more noticeable in bond distances than in BCP properties.

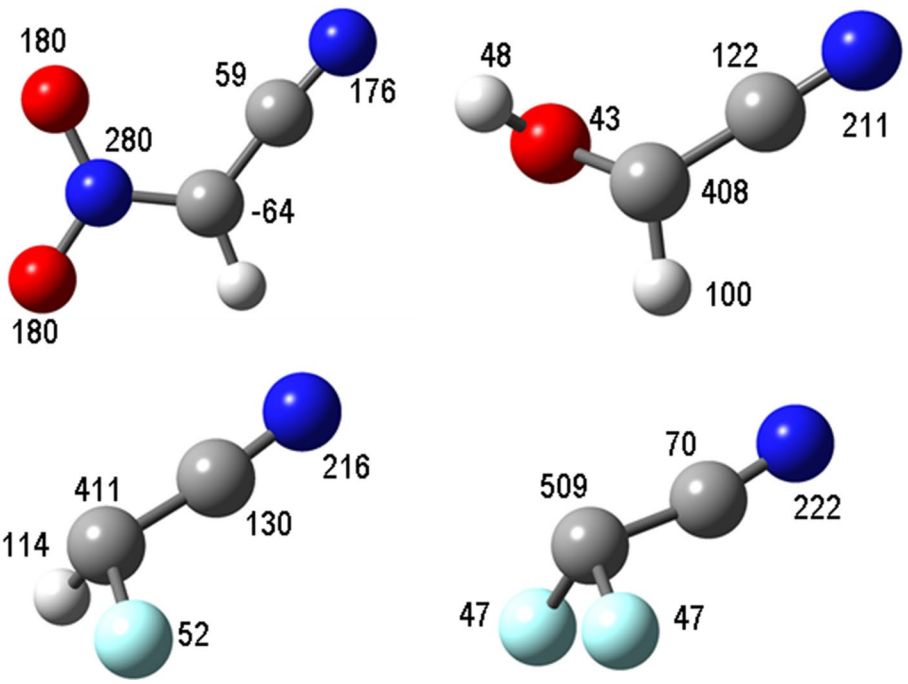

Fig. 6 $\Delta N(\Omega)$ values (in au multiplied by 10^3) upon α-deprotonation for compounds **5** (upside left), **6** (upside right), **10** (below left) and **11** (below right)

Table 3 Variations of most significant BCP properties upon α-deprotonation in compounds **5**, **6**, **9**, and **10**

		$\Delta\varepsilon$	$10^3\Delta\rho(\boldsymbol{r}_c)$/au	$10^3\Delta H(\boldsymbol{r}_c)$/au	$10^3\Delta R$/Å
5	C≡N	0.036	− 13.9	44.0	17
	C^{α}-C(N)	0.221	25.5	− 65.1	− 59
	C^{α}–H	0.070	− 0.1	− 5.6	− 14
	C^{α}–R; R=NO_2	0.476	75.2	− 249.6	− 162
	N–O	− 0.011	− 57.6	141.2	48
6	C≡N	0.038	− 24.6	76.8	27
	C^{α}-C(N)	0.279	34.8	− 86.8	− 77
	C^{α}-H	0.089	− 9.4	6.8	− 7
	C^{α}-R; R=OH	0.205	− 43.0	79.3	53
	O–H	0.004	10.9	− 8.1	− 6
10	C≡N	0.038	− 23.3	72.6	26
	C^{α}-C(N)	0.254	27.5	− 73.2	− 66
	C^{α}-H	0.084	− 12.7	14.0	− 3
	C^{α}-R; R=F	0.339	− 51.6	107.6	73
9	C≡N	0.025	− 20.2	64.1	23
	C^{α}-C(N)	0.175	29	− 75.8	− 64
	C^{α}-H	0.036	− 6.3	2.2	− 8
	C^{α}-R; R=SiH_3	0.203	19.6	− 16.4	− 114
	Si-H^g	0.021	− 10.4	10.2	31
	Si-H^a	0.022	− 8.3	9.0	19

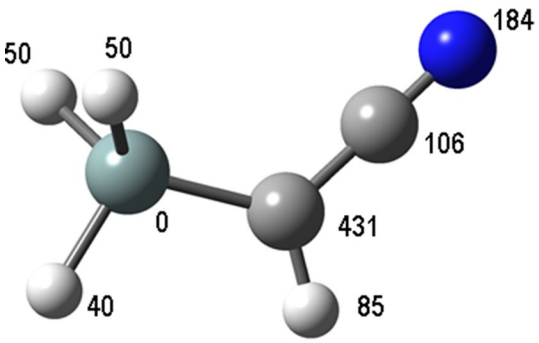

Fig. 7 $\Delta N(\Omega)$ values (in au multiplied by 10^3) upon α-deprotonation for compound **9**

2.5 Deprotonation effects on atomic electron populations and bond properties in nitriles containing π-conjugated units

The effects introduced by attaching vinyl (**16**), allyl (**17**) or (un)substituted phenyl groups (**18**–**24**) to the CH_2CN unit were also studied. As a general rule, these groups receive more electron density in the anion than alkyl groups (Table 4). Some trends can be established for the variation of atomic and group population upon α-deprotonation (Table 4) in this set of compounds: (i) The electron population gained by the $C^{\alpha}H$ unit reduces significantly with regard to alkyl compounds, always more than 0.1 au. This reduction mainly affects to C^{α}; (ii) the electron density transferred to the CN group reduces more with phenyl groups than with allyl and vinyl ones, and the amount of this reduction depends on the substitution of the phenyl group.

Vinyl and allyl groups are the only cases where $\Delta N(C^{\beta})$ is positive. For all the phenyl groups here studied, this atom reduces its electron population when a proton is extracted from its attached C^{α}. The reorganization of the electron density in the aromatic ring depends on the nature and position of the substituent. We notice some discrepancies with the predictions of the resonance model. Thus, the electron density gained by *meta*-CHs is larger in **18** than that taken by *orto*-CHs.

The analysis of BCP properties (data not shown) reveals, as expected from the RM, the reinforcement of C^{α}–C^{β} bond, showing larger $\rho(\boldsymbol{r}_c)$ values and shorter lengths.

3 Conclusions

QTAIM analysis of the electron densities of 24 substituted cyanocompounds and the corresponding anions obtained upon deprotonation allowed us to establish the following conclusions: α-deprotonation is at least favored by 100 kJ mol^{-1} with regard to other deprotonation processes. While resonance electron attractors reduce significantly the energy involved in the process, the effect of resonance electron donors is nearly negligible. Deprotonation involves a significant variation of atomic electron populations. Whereas hydrogen atoms are involved in this rearrangement, the role they play is not so important as that in protonation. In contrast, those atoms where the resonance model predicts significant delocalizations of the negative charge gain an important part of the electron density left by the hydrogen. Nevertheless, the evolution of electron density in this process is not completely explained by the resonance model. A detailed analysis of electron delocalization could be carried out in future research by using QTAIM delocalization indices and/or electron localization-delocalization matrices (LDMs).

Table 4 Variation of atomic and group electron population upon α-deprotonation of compounds **15–22**

	15	16[a]	17	18	19	20	21	22
CN	351	311	294	257	187	259	239	254
$C^{\alpha}H$	370	268	267	264	202	270	239	259
R	252	362	364	431	555	429	461	441
N(CN)	194	199	171	149	111	147	143	149
C^{α}	268	268	177	177	134	190	158	173
C^{ipso}	− 30	115	167	− 29	− 21	− 32	− 25	− 28
$C^{o}H$	–	–	–	162	158	153	148	138
$C^{m}H$	–	–	–	166	134	150	94	149
$C^{p}H$	–	–	–	132	− 64[b]	106	115	116
NO_2/NH_2	–	–	–	–	349	78	129	65
$N(NO_2/NH_2)$	–	–	–	–	146	− 32	37	− 19

All values in au multiplied by 10^3

[a]Compound 16 does not present a hydrogen atom attached to C^{α}

[b]There is no H attached to C^{p} in this compound

Acknowledgements We are indebted to "Centro de Supercomputación de Galicia" (CESGA) for access to their computational facilities and "Xunta de Galicia" for financial support.

Author contributions All the authors have shared the tasks involved in this work.

Funding Open Access funding provided thanks to the CRUE-CSIC agreement with Springer Nature. Partially funded by "Xunta de Galicia" with GRC 2019/24. F.T. stay in Vigo was partially funded by Iacobus Program.

Data availability There is no supplementary information available for this work. All the data presented in tables and figures were obtained by the authors.

Declarations

Conflict of interest The authors declare that there are no conflicts of interest.

Consent to participate and for publication Not applicable.

References

1. Knochel P, Molander GA (2014) Comprehensive organic synthesis. Elsevier, Amsterdam
2. Richard JP (1990) In: Rappoport Z (ed) The Chemistry of Enols. Wiley, New York
3. Carey FA, Sundberg RJ (2001) Advanced organic chemistry. Kluwer Academic, New York
4. Wheland GW (1955) Resonance in organic chemistry. Wiley, New York
5. Ferro-Costas D, Mosquera RA (2015) Excluding hyperconjugation from the Z conformational preference and investigating its origin: formic acid and beyond. Phys Chem Chem Phys 17:7424–7434. https://doi.org/10.1039/c5cp03805g
6. Wiberg KB, Laidig KE (1987) Barriers to rotation adjacent to double bonds. 3. The carbon-oxygen barrier in formic acid, methyl formate, acetic acid, and methyl acetate. The origin of ester and amide resonance. J Am Chem Soc 109:5935–5943. https://doi.org/10.1021/ja00254a006
7. Wiberg KB, Breneman CM (1992) Resonance interactions in acyclic systems. 3. Formamide internal rotation revisited. Charge and energy redistribution along the C–N bond rotational pathway. J Am Chem Soc 114:831–840. https://doi.org/10.1021/ja00029a005
8. Slee TS, MacDougall PJ (1988) The correspondence between Hückel theory and ab initio atomic charges in allyl ions. Can J Chem 66:2961–2962. https://doi.org/10.1139/v88-459
9. Laidig KE (1992) Use of nuclear potential to investigate the atomic size dependency of populations defined within the theory of atoms in molecules. J Am Chem Soc 114:7912–7913. https://doi.org/10.1021/ja00046a047
10. Laidig KE, Cameron LM (1996) Barrier to rotation in thioformamide: implications for amide Resonance. J Am Chem Soc 118:1737–1742. https://doi.org/10.1021/ja952678y
11. Glaser R (1989) Diazonium ions: a theoretical study of pathways to automerization, thermodynamic stabilities, and topological electron density analysis of the bonding. J Phys Chem 93:7993–8003. https://doi.org/10.1021/j100361a009
12. Glaser R, Choy GSC. Importance of the anisotropy of atoms in molecules for the representation of electron density distributions with Lewis structures. A case study of aliphatic diazonium ions. J Am Chem Soc. 115:2340–2347 https://doi.org/10.1021/ja00059a031.
13. Speers P, Laidig KE, Streitwieser A (1994) Origins of the acidity trends in dimethyl sulfide, dimethyl sulfoxide, and dimethyl sulfone. J Am Chem Soc 116:9257–9261. https://doi.org/10.1021/ja00099a049

14. Vila A, Mosquera RA (2001) Electron density analysis of small ring ethers. Tetrahedron 57:9415–9422. https://doi.org/10.1016/S0040-4020(01)00946-2
15. González Moa MJ, Mosquera RA (2003) Applicability of resonance forms in pyrimidinic bases. An AIM study. J Phys Chem A 107:5361–5367. https://doi.org/10.1021/jp034451s
16. González Moa MJ, Mosquera RA (2005) On the applicability of resonance forms in pyrimidinic bases. II. QTAIM interpretation of the sequence of protonation affinities. J Phys Chem A 109:3682–3686. https://doi.org/10.1021/jp044529k
17. González Moa MJ, Mandado M, Mosquera RA (2006) Explaining the sequence of protonation affinities of cytosine with QTAIM. Chem Phys Lett 428:255–261. https://doi.org/10.1016/j.cplett.2006.07.073
18. López JL, Graña AM, Mosquera RA (2009) Electron density analysis on the protonation of nitriles. J Phys Chem A 113:2652–2657. https://doi.org/10.1021/jp811023x
19. Mandado M, Van Alsenoy C, Mosquera RA (2004) Comparison of the AIM and Hirshfeld totals, σ, and π charge distributions: a study of protonation and hydride addition processes. J Phys Chem A 108:7050–7055. https://doi.org/10.1021/jp049338w
20. Graña AM, Hermida-Ramón JM, Mosquera RA (2005) QTAIM interpretation of the basicity of substituted anilines. Chem Phys Lett 412:106–109. https://doi.org/10.1016/j.cplett.2005.06.096
21. Mandado M, Mosquera RA, Graña AM (2004) AIM interpretation of the acidity of phenol derivatives. Chem Phys Lett 386:454–459. https://doi.org/10.1016/j.cplett.2004.01.084
22. Mandado M, Van Alsenoy C, Mosquera RA (2005) Electron charge redistribution upon hydride addition to carbonylic compounds. Chem Phys Lett 405:10–17. https://doi.org/10.1016/j.cplett.2005.02.011
23. Mandado M, Van Alsenoy C, Mosquera RA (2005) Joint QTAIM and hirshfeld study of the σ and π charge distribution and electron delocalization in carbonyl compounds: a comparative study with the resonance model. J Phys Chem A 109:8624–8631. https://doi.org/10.1021/jp051953s
24. Otero N, González Moa MJ, Mandado M, Mosquera RA (2006) QTAIM study of the protonation of indole. Chem Phys Lett 428:249–254. https://doi.org/10.1016/j.cplett.2006.07.059
25. Otero N, Estévez L, Mandado M, Mosquera RA (2012) An electron-density-based study on the ionic reactivity of 1,3-azoles. Eur J Org Chem 12:2403–2413. https://doi.org/10.1002/ejoc.201101407
26. Estévez L, Mosquera RA (2008) Where is the positive charge of flavylium cations? Chem. Phys. Lett. 451:121–126. https://doi.org/10.1016/j.cplett.2007.11.065
27. Bader RFW (1990) Atoms in Molecules: A Quantum Theory. Oxford University Press, New York
28. Bader RFW (1991) A quantum theory of molecular structure and its applications. Chem Rev 91:893. https://doi.org/10.1021/cr00005a013
29. Alcoba DR, Lain L, Torre A, Bochicchio RC (2005) Treatments of non-nuclear attractors within the theory of atoms in molecules. Chem Phys Lett 407:379–383. https://doi.org/10.1016/j.cplett.2005.03.078
30. Frisch MJ, Trucks GW, Schlegel HB, Scuseria GE, Robb MA, Cheeseman JR, Scalmani G, Barone V, Mennucci B, Petersson GA, Nakatsuji H, Caricato M, Li X, Hratchian HP, Izmaylov AF, Bloino J, Zheng G, Sonnenberg JL, Hada M, Ehara M, Toyota K, Fukuda R, Hasegawa J, Ishida M, Nakajima T, Honda Y, Kitao O, Nakai H, Vreven T, Montgomery JA Jr, Peralta JE, Ogliaro F, Bearpark M, Heyd JJ, Brothers E, Kudin KN, Staroverov VN, Kobayashi R, Normand J, Raghavachari K, Rendell A, Burant JC, Iyengar SS, Tomasi J, Cossi M, Rega N, Millam JM, Klene M, Knox JE, Cross JB, Bakken V, Adamo C, Jaramillo J, Gomperts R, Stratmann RE, Yazyev O, Austin AJ, Cammi R, Pomelli C, Ochterski JW, Martin RL, Morokuma K, Zakrzewski VG, Voth GA, Salvador P, Dannenberg JJ, Dapprich S, Daniels AD, Farkas Ö, Foresman JB, Ortiz JV, Cioslowski J, Fox DJ (2016) Gaussian09 revision D.01. Gaussian Inc, Wallingford CT.
31. Bader RFW. AIMPAC: a suite of programs for the AIM theory. Mc Master University, Hamilton, Ontario, Canada.
32. Aray Y, Murgich J, Luna MA (1991) Substituent effects and the charge topology in nitriles and cyanides. J Am Chem Soc 113:7135–7143. https://doi.org/10.1021/ja00019a008